# Graded wavelength one-dimensional photonic crystal reveals spectral characteristics of enhanced fluorescence

Patrick C. Mathias, Nikhil Ganesh, Wei Zhang, and Brian T. Cunningham[a)]
*Nano Sensors Group, Micro and Nanotechnology Laboratory, University of Illinois at Urbana-Champaign, 208 N. Wright Street, Urbana, Illinois 61801, USA*

(Received 18 December 2007; accepted 3 March 2008; published online 12 May 2008)

One-dimensional photonic crystal (PC) slabs are capable of enhancing the excitation of fluorescent material adsorbed on their surface. In this report, we demonstrate and verify by electromagnetic computer simulations that resonant leaky modes spectrally overlapping the laser wavelength used for fluorescent excitation are responsible for the enhanced excitation, and that the *Q*-factor of the PC resonance is proportional to the resonant electric field intensity and thus proportional to the fluorescent enhancement factor. As a demonstration, we have fabricated a single PC slab surface with an intentional spatial gradient in the resonant wavelength and demonstrate enhanced fluorescence only from locations on the PC surface with a leaky mode corresponding to a 633 nm HeNe laser used to excite Cyanine 5 dye deposited uniformly across the PC. The results show that enhanced fluorescence signals for one-dimensional PC slabs originate from increased excitation of the fluorescent dye. © *2008 American Institute of Physics*. [DOI: 10.1063/1.2917184]

## I. INTRODUCTION

The use of fluorophores for visualization and quantification of biomolecules is vital to life science procedures such as imaging of cells and cellular components and gene expression profiling.[1,2] The importance of fluorescence to the scientific community has motivated the engineering of optically active structures capable of enhancing the observed fluorescence of these molecules. While some research concerning the effects of metals on enhancing fluorescence appeared as early as the 1980s,[3–5] enhanced fluorescence research has gained momentum in recent years as the ease with which nanoscale structures can be constructed has increased. For example, metal-enhanced fluorescence that relies on surface plasmon resonance has been reported to increase the excitation of fluorophores,[6] to couple fluorophore emission into the far-field,[7,8] to alter the radiative decay rate of fluorophores,[9] and to employ some combination of these processes.[10–15] However, enhanced fluorescence on metal substrates can suffer from nonuniform enhancement when colloidal metal nanoparticles serve as the substrate. Patterned metal nanostructures alleviate this problem, but to date have not been fabricated over areas large enough to carry out biologically relevant experiments such as DNA microarrays. Metal substrates also are known to promote quenching when the fluorophore is within 20 nm of the substrate.[16]

Photonic crystals (PCs) have also demonstrated the capability to enhance fluorescence through mechanisms analogous to those observed with metal nanostructures, but since the structures are composed of dielectric materials, they will not promote quenching of fluorophores close to the PC surface. The PCs under study by our group are composed of a periodically modulated dielectric slab coated with a layer of high refractive index material (such as $TiO_2$), which can be fabricated uniformly over areas as large as microtiter plates. These PCs support guided-mode resonances, which are manifested as narrow-band reflections with spectral properties determined by the PC dimensions and materials. A guided-mode resonance occurs when light interacting with the structure couples to leaky modes, with which the reflected zeroth order undergoes total constructive interference and the transmitted zeroth order undergoes total destructive interference. For normally incident light, the result of this process is a nearly 100% efficient reflection occurring at a polarization-dependent wavelength, defined as the resonant wavelength.[17,18] At resonance, a constructive interference occurs within the high-index dielectric layer of the structure, resulting in heightened electric fields throughout the structure and its surface.[19,20] The increased intensity of the electric near-fields can translate into an increased excitation of fluorophores near the PC surface. Since the resonant condition may be fulfilled for a wide range of wavelengths or a wide range of incident light angles via phase matching,[21] the resonant wavelength for a PC structure can be tuned by adjusting the angle of incidence of light exciting the structure. Our group has recently used this principle to study two-dimensional PC surfaces that enhance fluorescence from Cyanine 5 (Cy5) (Ref. 22) as well as colloidal semiconductor quantum dots.[23] However, a clear demonstration of the resonant wavelength dependence of enhanced fluorescence for a fixed angle of incidence has not yet been performed.

One-dimensional PC surfaces have also demonstrated enhanced fluorescence[24,25] and offer a promising platform to study the dependence of enhanced fluorescence on resonant wavelength since they are simpler to characterize computationally. In this report, we demonstrate a one-dimensional PC in which the resonant wavelength of the device varies with position at a fixed illumination angle, allowing a single microscope-slide-sized device to exhibit resonances at a range of wavelengths including a fluorophore's excitation

a)Author to whom correspondence should be addressed. Electronic mail: bcunning@uiuc.edu.

 

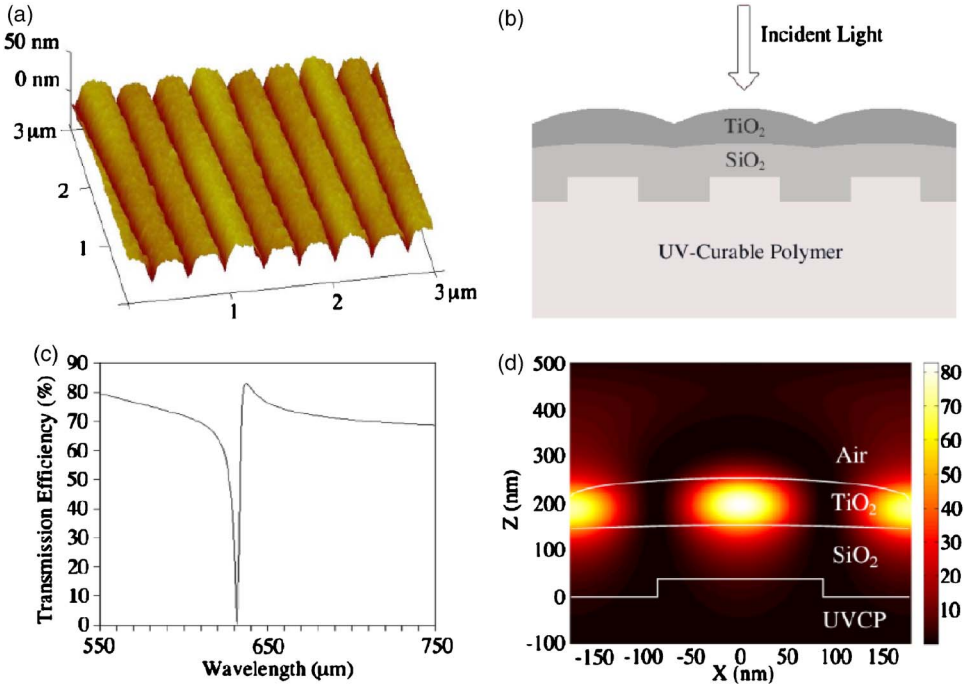


FIG. 1. (Color online) (a) Atomic force microscopy image of a portion of the photonic crystal surface. (b) Side view of the model used in Rigorous Coupled-Wave Analysis computations of the structure response. Dimensions are based on data from AFMs of the structure at various steps in fabrication. The structure period was 360 nm. The grating height was 60 nm, the $SiO_2$ height was 145 nm, and the $TiO_2$ thickness was varied from 70 to 220 nm. (c) Simulated transmission response as a function of wavelength under TE illumination for a region of the structure resonant at 633 nm. (d) Simulated electric field intensity for the structure in (b) when illuminated with 633 nm TE-polarized light at normal incidence.

wavelength. This is accomplished by depositing a high refractive index $TiO_2$ layer that varies in thickness over the length of the PC. By coating the device with a monolayer of Cy5-conjugated protein and scanning it at normal incidence with a microarray scanner, a spatial map of enhanced fluorescence can be generated to determine the resonant wavelength that corresponds to the greatest enhancement. The graded resonant wavelength device allows one to study this relationship at a high wavelength resolution that cannot be achieved unless a very large number of devices are fabricated with very small variations in the PC dimensions.

## II. EXPERIMENT AND SIMULATION

### A. Fabrication

The one-dimensional photonic crystal structure was fabricated with a nano-replica molding process previously used to generate plastic photonic crystal biosensors[26] and near-UV reflectance filters.[27] An 8 in. silicon master containing a pattern for a one-dimensional grating structure was fabricated using deep-UV lithography. A few drops of liquid polymer ($n_P$=1.46) were dispensed between the master and a sheet of polyethylene terephthalate (PET), distributed evenly to a thin film with a roller, and cured. The hardened polymer structure was then peeled off from the master. In addition to the PC structure, the replica also included an unpatterned flat surface to serve as a reference for enhanced fluorescence measurements. The patterned polymer absorbs a range of wavelengths of visible light and exhibits fluorescence throughout a wide range of visible wavelengths. Since the highest intensity electric fields at resonance occur within the high refractive index dielectric layer, it is advantageous to separate the high fields from the polymer via a $SiO_2$ spacer layer (which has the same refractive index as the polymer). A 145 nm layer of $SiO_2$ (measured by spectroscopic ellipsometry) with $n_{SiO_2}$=1.46 was deposited onto the structure by electron beam deposition (Denton Vacuum) to prevent excitation of fluorescence from the patterned polymer. This ensures that the fluorescent signal measured during illumination with the laser can be attributed primarily to the fluorescent dye and not to the polymer beneath the structure. After deposition of the spacer, a graded layer of $TiO_2$ ($n_{TiO_2}$=2.30) was deposited onto the structure by positioning the device in the sputter chamber (Cooke) such that various positions of the device were at different distances from the sputter source. The thickness of the $TiO_2$ film ranged from 70 to 220 nm over a distance of 60 mm. The PET substrate on which the graded wavelength photonic crystal was fabricated was then mounted on a glass microscope slide using an optical adhesive.

### B. Simulation

The behavior of the device was simulated using commercial software that employs Rigorous Coupled-Wave Analysis (RCWA, R-Soft DiffractMOD).[28] To determine the dimensions of the structure, atomic force microscopy was carried out on the structure surface after deposition of $TiO_2$ [Fig. 1(a)]. A model of the structure was then generated with these dimensions [Fig. 1(b)], and the simulated response of the structure was computed upon illumination with normally incident TE-polarized light (polarization parallel to grating lines). Illuminating with broadband incident light, the transmission efficiency as a function of wavelength was simulated for the range of $TiO_2$ thicknesses observed on the actual PC device. A representative plot of transmission efficiency as a function of wavelength for one thickness of $TiO_2$ is shown in Fig. 1(c). To assist in quantifying the effect that enhanced electric near-fields would have on enhanced fluorescence, the electric field profile of the structure during normally incident illumination with 633 nm TE light (the wavelength and polarization of the fluorescence scanner light source) was simu-

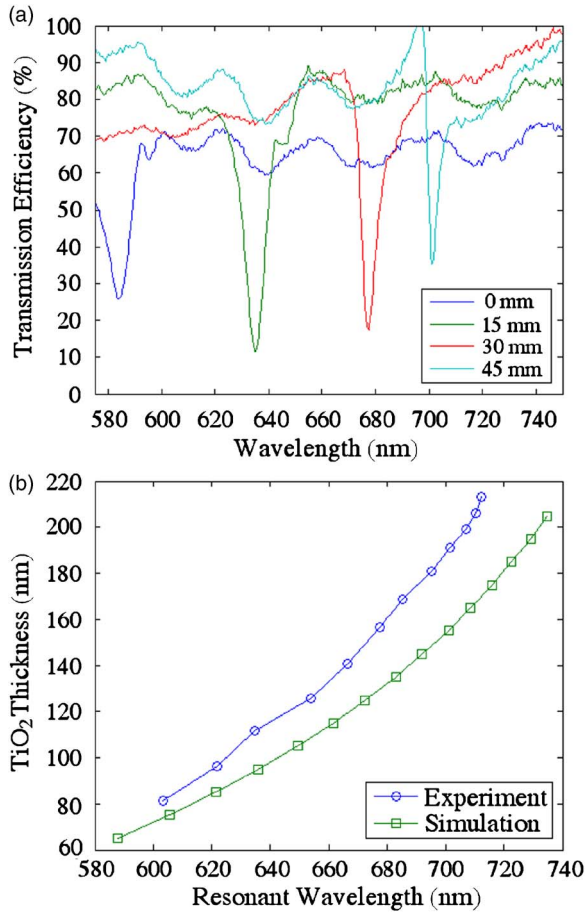


FIG. 2. (Color online) (a) Sample transmission spectra from four locations on the graded wavelength photonic crystal at near-normal incidence. (b) Resonant wavelength as a function of position for the actual graded wavelength photonic crystal and for a simulated structure.

lated for the range of $TiO_2$ thicknesses observed experimentally, and the results were complied for later analysis. A representative plot of the electric near-fields when the resonant condition is fulfilled appears in Fig. 1(d). The electric field intensity in the high-index $TiO_2$ layer is high relative to the incident light, with a maximum intensity of 80 times that of the incident light intensity. This region of enhanced near-fields extends above the surface of the structure, which would allow it to interact with immobilized fluorophores. The high field region is also pulled away from the patterned polymer by the $SiO_2$ layer, minimizing the background fluorescence observed from the structure.

### C. Spectral measurements

The resonant wavelength was then measured as a function of position on the device, along the direction of the $TiO_2$ gradient. Broadband white light was expanded and collimated from a fiber and passed through a polarizer to isolate the TE polarization before illuminating the device. The light transmitted through the device was fed to a UV-visible light spectrometer and the transmission spectra were collected. Spectra were collected for 13 locations throughout the device, with each location separated by a distance of 5 mm. Several sample spectra are overlaid in Fig. 2(a). These spectra all exhibit a clear dip in the transmission efficiency at a position-dependent wavelength. Using the ellipometry data detailing the $TiO_2$ thickness at each position on the device, the resonant wavelengths are plotted as a function of $TiO_2$ thickness in Fig. 2(b). The simulated dependence of resonant wavelength on $TiO_2$ thickness also appears in this figure. The two curves follow the same trend, although the experimental resonant wavelengths are increasingly lower than those predicted by simulation as the $TiO_2$ thickness increases. This may be explained by the fact that the simulation does not take into account the increased rounding of the structure as the $TiO_2$ thickness increases, nor does it take into account the dispersion in the refractive index of $TiO_2$.

### D. Fluorescence measurements

The capability of the device to exhibit enhanced fluorescence was tested by applying a uniform monolayer of fluorescently labeled protein onto the entire PC surface. The device surface was functionalized using a 5 min incubation with 3-aminopropyltriethoxy-silane (Pierce) in dry acetone, followed by a 2 h incubation with 25% glutaraldehyde (Sigma Aldrich). The deposition of protein was completed with a 15 h incubation with a 100 $\mu$g/ml solution of Cy5-conjugated streptavidin (GE Healthcare, excitation peak at 649 nm, emission peak at 670 nm) followed by a wash with 0.05% Tween (Sigma Aldrich) and a 5 min ultrasonication in deionized water. The dye-coated device was then imaged at 20 $\mu$m resolution with a microarray scanner (Tecan LS Reloaded) at normal incidence and an excitation wavelength of 633 nm [Fig. 3(a)]. The incident light has a fixed polarization, which in this case is the TE polarization specified in simulation. A line profile from the fluorescence image along the $TiO_2$ gradient was taken both on and off of the photonic crystal surface [Figs. 3(b) and 4(a)], to be compared with the simulated data for the distribution and amplitudes of the electric near-fields. The spatial position for the image and the line profiles was translated into $TiO_2$ thickness using a linear equation derived from the ellipsometry data.

To convert the simulation data into a format compatible with the experimental fluorescence line profiles, the electric field intensities observed when the device is illuminated were derived from the normalized simulated electric field profiles. The electric field intensities from the top surface of the PC were spatially averaged for a single period for each thickness of $TiO_2$ simulated. The averaged electric field intensity values were then plotted as a function of $TiO_2$ thickness [Figs. 3(c) and 3(d)]. The procedure was repeated for the thin-film condition in which no PC structure was present [Fig. 4(b)].

## III. RESULTS AND DISCUSSION

The fluorescence line profile on the PC shows a dramatic increase in the fluorescence signal on the region of the chip where the $TiO_2$ thicknesses are between 90 and 120 nm [Fig. 3(b)]. Specifically, the first peak, with a higher intensity and a smaller peak width, appears at a $TiO_2$ thickness of approximately 100 nm. The maximum fluorescence intensity at this location is approximately 24 400 counts (cts). A second peak appears at a $TiO_2$ thickness of 110 nm, with a maximum

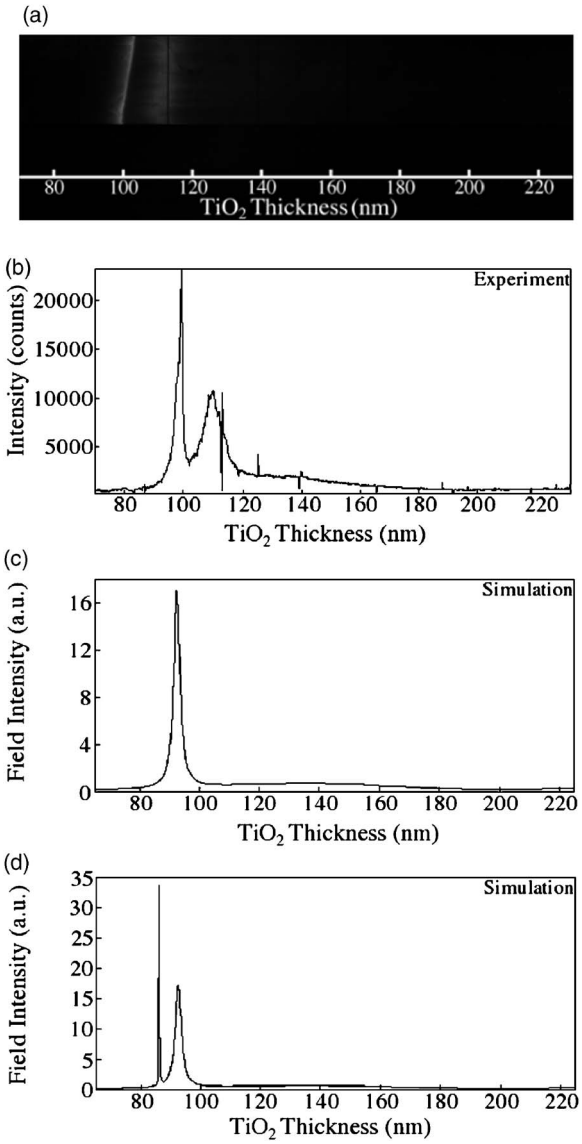


FIG. 3. (a) Fluorescence image of the entire graded wavelength photonic crystal device after application of a Cyanine-5 conjugated streptavidin monolayer. (b) Line profile from one horizontal line spanning the photonic crystal on the fluorescent image. (c) Simulated average electric field intensity on the top surface of the photonic crystal under normally incident 633 nm TE-polarized illumination, for the range of $TiO_2$ thicknesses deposited on the actual structure. (d) Simulated average electric field intensity as in (c), with an angle of incidence of 0.25°.

intensity of approximately 11 000 cts. This range of locations corresponds to the region in which the PC resonant wavelength overlaps the excitation wavelength of the laser (633 nm), but the appearance of two peaks is not predicted by the simulated electric field intensity for normally incident 633 nm TE-polarized light [Fig. 3(c)]. Displaying two peaks, however, is typical behavior for PCs supporting guided-mode resonances when the angle of incidence deviates from normal; this occurs because two wavelengths rather than one fulfill the resonant condition.[21] By varying the angle of incidence of the excitation light in simulation, two peaks can be observed in the plot of average electric field intensity as a function of $TiO_2$ thickness. Figure 3(d) shows the field intensity plot when the incidence angle is altered by only 0.25° from normal incidence, which could occur if the height on

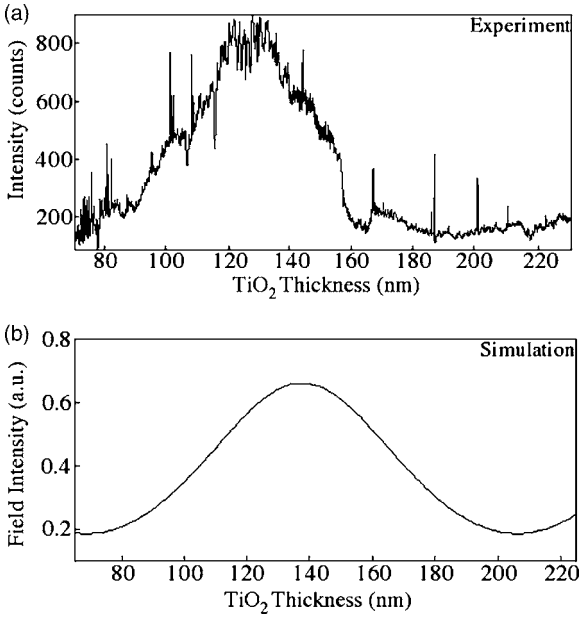


FIG. 4. (a) Line profile from one horizontal line spanning the region of the device without a photonic crystal on the fluorescent image. (b) Simulated average electric field intensity on the top surface of the off-device region under normally incident 633 nm TE-polarized illumination, for the range of $TiO_2$ thicknesses deposited on the actual structure.

the two edges of the slide differed by only 130 $\mu$m. The process of mounting the PC by hand using optical adhesives can introduce such errors. Two peaks are observed with a higher intensity peak preceding a lower intensity peak, which reflects the trend observed in the experimental data. The two peaks in the simulation data differ in $TiO_2$ thickness by 8.5 nm, and the two peaks observed experimentally show a difference in $TiO_2$ thickness of approximately 10 nm.

The fluorescent line profile for the region off the photonic crystal exhibits a sinusoidal variation in intensity as the $TiO_2$ thickness is varied [Fig. 4(a)]. This behavior is predicted by simulation [Fig. 4(b)] and occurs due to thin film interference effects. While the raw data from this surface may serve as a reference if a fixed position on the device is adopted, such a reference value would not reflect a fluorescence measurement carried out on an optically passive surface such as glass. Thus a true value for fluorescence intensity (assuming a passive surface is used) must be derived. This can be accomplished by correlating the maximum and minimum intensity values of the simulated electric field [Fig. 4(b)] with the maximum and minimum values for the fluorescence line profile [Fig. 4(a)]. This analysis would suggest the fluorescence intensity would be approximately 1350 cts in the absence of the dielectric thin film (if the electric field intensity was 1), which can be adopted as a reference value from which to determine the enhancement factor. While the assay could be carried out on a glass slide to serve as a reference, it is important to note that the silanization procedure would yield different results on a glass surface rather than a $TiO_2$ surface, confounding the comparison.

To gain a clearer understanding of why two peaks of fluorescent intensity occur rather than one, the device transmission due to white light illumination was simulated at an incidence angle of 0.25° (Fig. 5). The transmission spectra

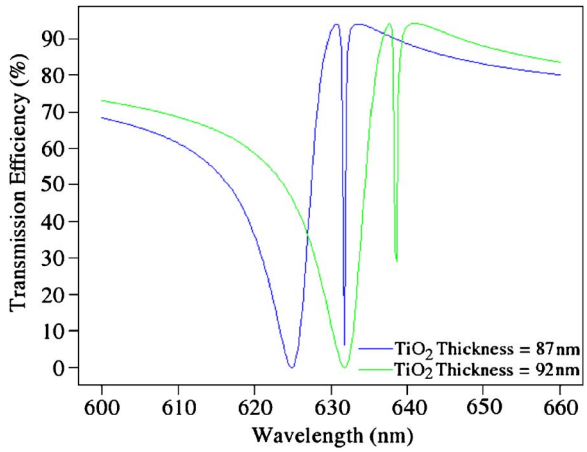


FIG. 5. (Color online) Simulated transmission at an incidence angle of 0.25° for two $TiO_2$ thicknesses (87 and 92 nm) at which distinct peaks exhibit minimum transmission at a wavelength of 633 nm.

for the device at two different $TiO_2$ thicknesses (87 and 92 nm) are plotted; for each of the thicknesses, two distinct reflection peaks (or transmission dips) are clearly observed in the response. At a thickness of 87 nm, a peak with a full-width at half-maximum (FWHM) of 0.3 nm is centered at 633 nm, and at a thickness of 92 nm, a peak with a FWHM of 11 nm is centered at the same wavelength. The lower $TiO_2$ thickness (87 nm), at which the peak with smaller line width (FWHM=0.3 nm) crosses the 633 nm excitation wavelength, is correlated with the simulated maximum enhancement of 34 times observed in Fig. 3(d). Analogously, the $TiO_2$ thickness of 92 nm (FWHM=11 nm) correlates with the simulated lower intensity peak showing an enhancement of 17 times. Taking into account the adjusted reference value for predicted fluorescent intensity on a passive surface, the maximum enhancement in the experimental data [Fig. 3(b)] is 18 times and enhancement from the lower intensity peak is 8 times. These values are approximately half of the simulated values, which may be the result of choosing a fixed position above the surface at which to average the field during simulation. In reality, the fluorophores are present at various heights above the surface. In addition, because the line widths of the experimental spectral peaks are difficult to evaluate, there may be deviations between these and the simulated resonant line widths that also account for the difference in enhancement factors.

Although the splitting of the resonance into two peaks was not originally anticipated, it provided a region of the device in which the simulated enhancement [Fig. 3(d)] was two times higher than that predicted in the normal incidence simulation [Fig. 3(c)]. The simulated data in Fig. 5 suggest that this increased enhancement stems from the generation of a peak with a low spectral width (FWHM=0.3 nm). Although the resolution of the spectrometer used to generate experimental transmission spectra cannot adequately resolve peaks of such low spectral width, the experimental data in Fig. 3(b) suggest that two peaks are present and one has a smaller spectral width than the other. These data verify that it is advantageous to design PC slabs for enhanced fluorescence such that resonances have small line widths that overlap the excitation wavelength of the incident light. However, the small line width of the fluorescence profile peak with larger intensity illustrates that only a small range of $TiO_2$ thicknesses can achieve maximal response. If one relies on a fluorescence scanner that has an excitation path fixed at normal incidence, the $TiO_2$ layer of the photonic crystal must be deposited at a precise thickness in order to align the resonance wavelength with the excitation wavelength. Furthermore, the addition of biomolecules on the device surface alters the effective refractive index of the structure, changing the resonant wavelength; this is the working principle behind photonic crystal biosensors.[29] This issue can be alleviated by using a fluorescence scanner with an adjustable angle of incidence, since the resonant condition for a specific wavelength is a function of angle. If this is not an option, the tradeoff between line width and enhancement factor must be assessed during the design of PCs for enhanced fluorescence.

The feasibility of this approach in performing enhanced fluorescence over areas as large as an entire microscope slide can be determined by evaluating tolerances of the system under study. At normal incidence, the relationship between the period of the photonic crystal and the wavelength at which it operates can be estimated by the following equation:

$$\lambda = n_{\text{eff}}\Lambda \tag{1}$$

in which $\lambda$ represents the wavelength at which the transmission dip occurs, $n_{\text{eff}}$ represents the effective refractive index of the resonant mode, and $\Lambda$ represents the period of the structure.[30] Using the measured wavelength of operation and period of the device, the effective refractive index can be approximated as 1.76. The fluorescent molecules are excited by a laser operating at a fixed wavelength (633 nm) and a narrow spectral width. Assuming the mode effective refractive index does not vary, detuning of the resonance from the laser wavelength is possible when there are variations in the photonic crystal period. By applying Eq. (1) and substituting $\Delta\lambda$, or the FWHM of the photonic crystal resonance, for the laser wavelength $\lambda$, an approximation of the tolerance in the period ($\Delta\Lambda$) can be obtained. This tolerance represents the change in period required to completely shift the resonance away from the laser wavelength. To obtain the maximum enhancement illustrated in this work, a FWHM of $\Delta\lambda = 0.3$ nm was required, which indicates that a change in period of 0.528 nm would be sufficient to shift the peak away from the target wavelength. An enhancement factor of eight times was achieved with a peak that had a FWHM of 11 nm. This translates to a much more favorable tolerance for the period of 19.4 nm. A change in period greater than 19.4 nm, or 5.38% of the period, would be required to shift the peak away from the target wavelength. It is important to note, however, that these calculations only apply to the materials used in this work, which determine the effective refractive index. This analysis also assumes a uniform $TiO_2$ thickness.

## IV. CONCLUSION

In conclusion, we have fabricated a photonic crystal with a graded thickness $TiO_2$ layer which contains reflective resonant peaks for a range of position-dependent wavelengths

spanning 100 nm. These resonances overlap a large range of wavelengths, including the excitation wavelengths for Cyanine 5. PC enhanced fluorescence is observed when a resonance overlaps the fluorophore excitation wavelengths. Our results also suggest that large enhancement factors can be achieved with PC designs in which the resonance has a small spectral line width.

## ACKNOWLEDGMENTS

This work was supported by SRU Biosystems and the National Science Foundation (Grant No. BES 0427657). The authors thank the staff of the Micro and Nano Technology Laboratory and colleagues from the Nano Sensors Group for their suggestions and input. Any opinions, findings, and conclusions or recommendations in this work are those of the authors and do not necessarily reflect the views of the National Science Foundation.

[1]T. Chishima, Y. Miyagi, X. Wang, H. Yamaoka, H. Shimada, A. R. Moossa, and R. M. Hoffman, Cancer Res. **57**, 2042 (1997).
[2]M. Schena, D. Shalon, R. W. Davis, and P. O. Brown, Science **270**, 467 (1995).
[3]P. Das and H. Metiu, J. Phys. Chem. **89**, 4680 (1985).
[4]W. R. Holland and D. G. Hall, Opt. Lett. **10**, 414 (1985).
[5]D. A. Weitz, S. Garoff, J. I. Gersten, and A. Nitzan, J. Chem. Phys. **78**, 5324 (1983).
[6]Y.-J. Hung, I. I. Smolyaninov, and C. C. Davis, Opt. Express **14**, 10825 (2006).
[7]K. Aslan, S. N. Malyn, and C. D. Geddes, J. Fluoresc. **17**, 7 (2007).
[8]K. Ray, H. Szmacinski, J. Enderlein, and J. R. Lakowicz, Appl. Phys. Lett. **90**, 251116 (2007).
[9]O. L. Muskens, V. Giannini, J. A. Sanchez-Gil, and J. G. Rivas, Nano Lett. **7**, 2871 (2007).
[10]Y. Chen, K. Munechika, and D. S. Ginger, Nano Lett. **7**, 690 (2007).
[11]Y. Fu and J. R. Lakowicz, J. Phys. Chem. B **110**, 22557 (2006).
[12]Y. Fu and J. R. Lakowicz, Anal. Chem. **78**, 6238 (2006).
[13]Y. Liu and S. Blair, Opt. Lett. **28**, 507 (2003).
[14]O. Stranik, H. M. McEvoy, C. McDonagh, and B. D. MacCraith, Sens. Actuators B **107**, 148 (2005).
[15]P. P. Pompa, L. Martiradonna, A. D. Torre, F. D. Sala, L. Manna, M. D. Vittorio, F. Calabi, R. Cingolani, and R. Rinaldi, Nat. Nanotechnol. **1**, 126 (2006).
[16]A. M. Glass, P. F. Liao, J. G. Bergman, and D. H. Olson, Opt. Lett. **5**, 368 (1980).
[17]R. Magnusson and S. S. Wang, Appl. Phys. Lett. **61**, 1022 (1992).
[18]S. S. Wang, R. Magnusson, J. S. Bagby, and M. G. Moharam, J. Opt. Soc. Am. A **7**, 1470 (1990).
[19]Y. Ding and R. Magnusson, Opt. Express **12**, 5661 (2004).
[20]C. Wei, S. Liu, D. Deng, J. Shen, J. Shao, and Z. Fan, Opt. Lett. **31**, 1223 (2006).
[21]R. Magnusson, Y. Ding, K. J. Lee, D. Shin, P. S. Priambodo, P. P. Young, and T. A. Maldonado, Proc. SPIE **5225**, 21 (2003).
[22]P. C. Mathias, N. Ganesh, L. L. Chan, and B. T. Cunningham, Appl. Opt. **46**, 2351 (2007).
[23]N. Ganesh, W. Zhang, P. C. Mathias, E. Chow, J. A. N. T. Soares, V. Malyarchuk, A. D. Smith, and B. T. Cunningham, Nat. Nanotechnol. **2**, 515 (2007).
[24]W. Budach, D. Neuschafer, C. Wanke, and S.-D. Chibout, Anal. Chem. **75**, 2571 (2003).
[25]D. Neuschafer, W. Budach, C. Wanke, and S.-D. Chibout, Biosens. Bioelectron. **18**, 489 (2003).
[26]B. Cunningham, B. Lin, J. Qiu, P. Li, J. Pepper, and B. Hugh, Sens. Actuators B **85**, 219 (2002).
[27]N. Ganesh and B. T. Cunningham, Appl. Phys. Lett. **88**, 071110 (2006).
[28]M. G. Moharam and T. K. Gaylord, J. Opt. Soc. Am. **71**, 811 (1981).
[29]B. Cunningham, P. Li, B. Lin, and J. Pepper, Sens. Actuators B **81**, 316 (2002).
[30]R. Magnusson, Y. Ding, K. J. Lee, D. Shin, P. S. Priambodo, P. P. Young, and T. A. Maldonado, Proc. SPIE **5225**, 20 (2003).